# Effects of Free Carriers on Zone-Center Vibrational Modes in Heavily Doped $p$-type Si. I. Acoustical Modes

Tor A. Fjeldly, Fernando Cerdeira, and Manuel Cardona
*Max-Planck-Institut für Festkörperforschung, 7000 Stuttgart 1, Federal Republic of Germany*
(Received 1 March 1973; revised manuscript received 11 June 1973)

We have performed a systematic study of free-carrier effects on the elastic constant $C_{44}$ (this paper) and on the Raman spectrum (a succeeding paper) of heavily doped $p$-type Si. We have considered samples with a wide range of impurity (boron) concentrations, with and without the application of uniaxial stress. The data on the acoustical modes are compared with Keyes's theory, and extensions of this containing the effects of an external uniaxial stress. In particular, we have found satisfactory agreement between experiments and theory in the regions of high and low impurity concentrations. The various calculations were based on models for the valence bands, yielding information as to their applicability to problems of this nature. More generally, we have found a number of similarities between the effects of doping on the acoustical and optical zone-center vibrational modes, suggesting that both effects are produced by the same basic mechanism.

## I. INTRODUCTION

It was shown by Keyes some years ago that the free carriers can produce significant contributions to certain elastic constants in heavily doped semiconductors.[1,2] The mechanism he proposed is, in short, as follows: The strain associated with an elastic wave may distort the bands and lift the degeneracy of the band extrema where the free carriers are contained, causing intraband and interband redistribution of carriers, respectively. This redistribution lowers the free energy of the strained crystal or, put in another way, part of the elastic energy is regained, thus effectively lowering the elastic constants.

In a number of experiments the correctness of this explanation has been confirmed; particularly in $n$-type materials, quantitative agreement with theory has been obtained,[1,3-6] largely due to the simple multivalley configuration to be considered in this case. In one experiment[7] it was shown that, with the application of a uniaxial stress, the electronic contribution to the elastic constant $C'$ in $n$-Si could be removed in a manner described satisfactorily by an extension of Keyes's theory. In $p$-type Ge and Si[1-3,6,8,9] the situation is less satisfactory, both from an experimental and a theoretical viewpoint. The theory is complicated by the fact that the free carriers are located at the valence-band edge at the Brillouin-zone center. The band structure is here quite involved, with a degeneracy between heavy- and light-hole bands at the $\Gamma$ point, and with a spin-orbit split-off band just below (these bands are hereafter referred to as h.h., l.h., and s.o., respectively). All three bands are warped, h.h. appreciably so; moreover, l.h. and s.o. are considerably nonparabolic.[10] On the experimental side only a few papers have appeared showing qualitative but not quantitative agreement with Keyes's theory. Recently a free-carrier effect similar to the one described here for the acoustical vibrations was observed by Cerdeira and Cardona[11] for the optical phonon frequencies in Ge and Si. Further information about the nature of electronic effect on all zone-center modes for these materials was obtained in an experiment with the sample subjected to uniaxial stress.[12] In that experiment it was suggested that an intimate relationship exists between the effects of doping on the acoustical and the optical modes. This arises from symmetry considerations, or more basically, from the similarity in the electron-phonon interaction terms.

The present investigation contains a systematic study of these and related electronic effects on the elastic constant (this paper) and on the Raman spectra[13] (the following paper, hereafter referred to as II) in heavily doped $p$-type Si. We have considered samples with a wide range of impurity (boron) concentrations, with and without the application of uniaxial stress. The Raman study was performed with several exciting laser wavelengths.[13] We compare the data with presently available theories to show the extent and the limitations of their validity.

In the present paper we first consider the variation of the elastic constant $C_{44}$ with carrier concentration ranging from $2.2\times10^{18}$ to $1.6\times10^{20}$ cm$^{-3}$. The results are compared with existing theories for the low-concentration and the high-concentration limits. With uniaxial stress along the [001] direction the degeneracy of the elastic constants $C_{44}$ and $C_{66}$ will be lifted, and experimentally their electronic contributions (hereafter referred to as $\Delta C_{44}$ and $\Delta C_{66}$, respectively) show qualitatively different stress dependences, in agreement with group theoretical considerations. A quantitative comparison is attempted by extending the above-

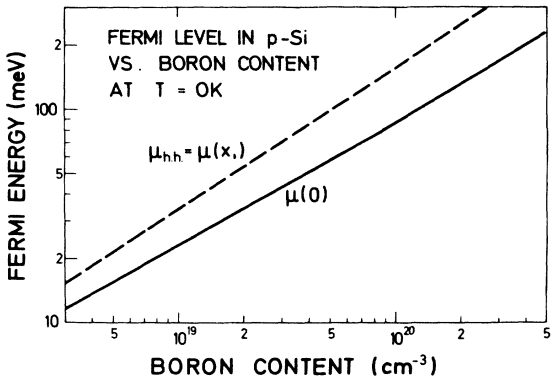


FIG. 1. Fermi energy vs carrier (hole) content for $p$-type Si, for zero stress $\mu(0)$ and for the [001] stress $X$, where the top of the l. h. passes through the Fermi surface, $\mu_{\text{h.h.}}=\mu(X_1)$.

mentioned theories for low and high concentrations to include the presence of either a very small or a very large uniaxial stress. Specifically, in the region of high stress, $X$, the electronic contributions are shown to vanish: $\Delta C_{44}$ as $X^{-1}$ and $\Delta C_{66}$ as $X^{-3}$.

## II. $\Delta C_{44}$, NO STRESS

### A. Experimental

The electronic contribution $\Delta C_{44}$ to the elastic constant $C_{44}$ was obtained by measuring the change in velocity (for a fast transverse wave propagating along [110]) in the doped samples relative to an intrinsic reference sample. For this experiment all samples (including the reference) were prepared in the same jig. The jig was a circular brass flat with holes on which each sample could be glued. The thickness of the jig was somewhat less than the desired crystal thickness, allowing both (110) end faces of the samples to be exposed for preparation. All samples were then carefully lapped and polished simultaneously to a thickness of $8.210\pm0.002$ mm and with a maximum deviation from parallelicity of $3\times10^{-5}$ cm/cm (~6 sec of arc). The crystal orientations were accurate to $\pm0.5°$.

The change in fast transverse velocity from that of the reference sample was measured by a pulse echo technique,[14] using a Matec rf pulse generator and receiver (model No. 6000). The pulses were excited by a 20-MHz $AC$ quartz transducer bonded to the sample by Nonaq stopcock grease. The measured velocity change versus impurity content is shown in Table I. This table also contains the relative change in elastic constant $\Delta C_{44}/C_{44}^i$ (superscript $i$ for intrinsic), where the value $C_{44}^i = 0.7951\times10^{12}$ dyn/cm$^2$ was taken from Ref. 5.

Table I further shows the Fermi energy [measured from the top of h. h. (l. h.)] as computed numerically from $\vec{k}\cdot\vec{p}$ bands. An average of the bands along all ⟨100⟩, ⟨111⟩, and ⟨110⟩ directions was used for this purpose, and the results are shown in Fig. 1. For details on this calculation we refer to Appendix A and Fig. 4.

### B. Theory

There exist, at present, tractable descriptions of the electronic effects on the elastic constants in the limit of small carrier concentration,[8] and in the high-concentration limit.[11] In these calculations one attempts to find the free energy to second order in the small ultrasonic strain. This free energy has the form[8]

$$\delta F=\sum_k f_k\,\delta E_k^{(2)}+\frac{1}{2}\sum_k\frac{\partial f_k}{\partial E_k}\,(\delta E_k^{(1)})^2\,, \tag{1}$$

where $f_k=(1+e^{(E_k-\mu)/k_BT})^{-1}$ is the Fermi distribution function for a state of wave vector $\vec{k}$. $\delta E_k^{(1)}$ and $\delta E_k^{(2)}$ are the changes in energy of state $\vec{k}$ to first and second order in the ultrasonic strains, respectively, and $\mu$ is the Fermi energy. The expression (1) is then compared to an equivalent expression in terms of the cubic elastic constants:

$$\begin{aligned}\delta F=&\tfrac{1}{2}\Delta C_{11}(\epsilon_{xx}^2+\epsilon_{yy}^2+\epsilon_{zz}^2)\\&+\Delta C_{12}(\epsilon_{xx}\epsilon_{yy}+\epsilon_{xx}\epsilon_{zz}+\epsilon_{yy}\epsilon_{zz})\\&+2\Delta C_{44}(\epsilon_{xy}^2+\epsilon_{xz}^2+\epsilon_{yz}^2)\,.\end{aligned} \tag{2}$$

For details on the calculation we refer to Sec. III

TABLE I. Change in fast transverse velocity for propagation along [110], and relative change in the elastic constant $C_{44}$ with doping (Fermi energy). $T=300$ K.

| Impurity content ($10^{19}$ cm$^{-3}$) | 0.22 | 0.6 | 1.5 | 2.6 | 7 | 16 |
|---|---|---|---|---|---|---|
| $\Delta v$ ($10^3$ cm/sec) | −0.1 | −0.5 | −2.0 | −3.4 | −7.7 | −13.4 |
| $\Delta C_{44}/C_{44}^i$ (%) | −0.09 | −0.23 | −0.74 | −1.22 | −2.66 | −4.53 |
| Fermi level $\lvert\mu\rvert$ (meV) | 9 | 17 | 29 | 40 | 69 | 114 |

and Appendix B, where this problem is treated on a more general basis including the stress dependence of $\Delta C_{44}$. We now consider the results for the low- and the high-concentration limits.

The low-concentration limit is defined by $\mu \ll \Delta_0$, where $\Delta_0 \simeq 44$ meV (for Si) is the spin-orbit splitting at the zone center. In this limit only l. h. and h. h. are populated by free carriers, and both of these bands can be taken to be parabolic. Bir and Tursunov's expression for this case is[8,11]

$$\left(\frac{\Delta C_{44}}{C_{44}}\right)_{LC} = -\left(\beta + (\tfrac{1}{2} - \beta)\frac{D^2}{15\overline{B}^2}\right)\frac{d^2}{2C_{44}}\frac{N}{k_B T}\frac{F'_{1/2}}{F_{1/2}} . \tag{3}$$

$d$ is a deformation potential constant; $\beta$, $D$, and $\overline{B}$ are valence-band parameters defined in Ref. 11. $F'_{1/2}(\mu/k_B T)$ and $F_{1/2}(\mu/k_B T)$ are the well-known Fermi integrals, and $N$ is the free-carrier (hole) concentration.

In their calculation of the high-concentration counterpart to Eq. (3) Cerdeira and Cardona[11] omitted a contribution to $\Delta C_{44}$ arising from the second term in Eq. (1). This contribution (increasing $|\Delta C_{44}|$ by about 16%) has been included here (see Sec. III), leading to the following high-concentration ($\mu \gg \Delta_0$) expression:

$$\left(\frac{\Delta C_{44}}{C_{44}}\right)_{HC} = -K\frac{d^2}{2C_{44}}\frac{N}{k_B T}\frac{F'_{1/2}}{F_{1/2}} , \tag{4}$$

where $K$ is a numerical constant ($K \simeq 0.69$), the origin of which is made clear in Appendix B. Equation (4) was obtained by approximating l. h. and h. h. by two parabolic bands (both with the h. h. mass $m_H$) which run parallel with a constant energy separation of $\frac{2}{3}\Delta_0$. The s. o. band was neglected since only a relatively small number of free carriers are contained in it (always less than 4%).

### C. Discussion

We note that the expressions (3) and (4) are the same except for a numerical factor. This suggests replacing the constant $K$ in Eq. (4) by a function $K(\mu)$, where $K(\mu)$ now can be regarded as a semiempirical function to be determined experimentally. Such a function can be useful in related free-carrier problems, where the complicated band structure makes accurate descriptions prohibitive. The experimentally obtained $K(\mu)$ is shown in Fig. 2 (filled circles), where for comparison, the actual numerical constant $K$ is also shown (dashed horizontal line) in both limits of concentration.

The experimental points agree reasonably with the calculations in the high-limit and low-limit case. The discrepancy is about what one should expect on the basis of the band approximations used.

## III. $\Delta C_{44}$ AND $\Delta C_{66}$ VERSUS [001] UNIAXIAL STRESS

As pointed out previously[7] a large uniaxial compression can split valley degeneracies ($n$-type case) and thus eliminate the effect of doping on the elastic properties, essentially confirming the electronic nature of the phenomenon. The corresponding effect in $p$-type Si[12] is to lift the h. h. – l. h. degeneracy at the zone center and for very high stresses, to eliminate the band distortions produced by the acoustical and optical vibrations.

In this section we present a study of the stress dependence of electronic effects on the elastic constant $C_{44}$ ($C_{66}$) for $p$-type Si in four samples ranging in Boron content from $6\times10^{18}$ to $1.6\times10^{20}$ cm$^{-3}$.

### A. Experimental

The stress apparatus used has been extensively discussed in the literature.[15,16] The samples were in the forms of square prisms with dimensions $2\times2\times17$ mm, with the long edges parallel to the [001] (stress) direction. $\Delta C_{44}$ and $\Delta C_{66}$ versus stress (compression) were measured as changes in the velocities for 30-MHz transverse waves propagating in the [100] direction (i.e., perpendicular to the stress). Under the action of the stress $C_{44}$ splits into a "singlet" $C_{66}$, which can be measured for an ultrasonic polarization perpendicular to the stress $X$, and a "doublet" $C_{44}$, which is obtained for a polarization parallel to $X$. Small (2×2-mm) 30-MHz $AC$ quartz transducers were bonded with epoxy to the (100) surfaces of the samples. Because of the presence of the transducers the samples usually broke at a stress of less than $9\times10^9$ dyn/cm$^2$. Reproducibility of the data with various samples from the same material, and with different size transducers, indicated that stress nonhomogeneities arising from the presence of the solidly bonded transducers did not mea-

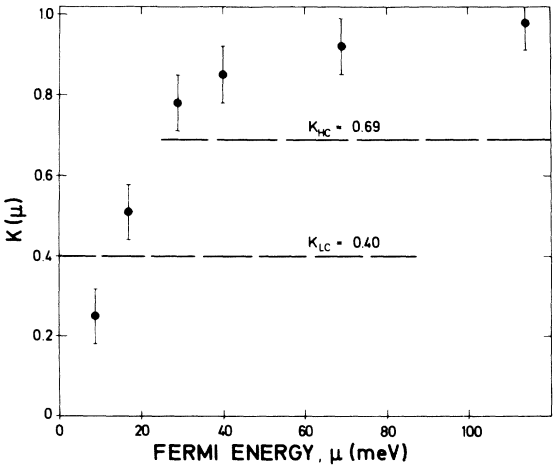


FIG. 2. Semiempirical function $K(\mu)$ (filled circles) compared with numerical estimates of $K$ in the high-concentration (HC) and in the low-concentration (LC) limits. Measured at 300 K.

surably influence the data obtained.

The results of these measurements, performed at liquid-nitrogen temperature, are presented in Fig. 3. The pure electronic effects were obtained by subtracting the stress dependence of the corresponding elastic constants for an intrinsic sample of the same dimensions (measured separately) from those found in the doped samples.

### B. Theory and Discussion

In this subsection we first present a group-theoretical argument for the qualitatively different stress dependences of $\Delta C_{44}$ and $\Delta C_{66}$, with special reference to the low-stress limit. Subsequently we present a calculation of the behavior of $\Delta C_{44}$ and $\Delta C_{66}$ in the extreme-high-stress limit showing that the electronic effects should disappear, thereby establishing a plausibility argument for the qualitative shape of the curves in Fig. 3. Finally we extend Keyes's theory to include the presence of a small external uniaxial stress.

The initial slopes of $\Delta C_{44}$ and $\Delta C_{66}$ versus stress (low-stress limit) can be qualitatively explained as follows (see also Ref. 12): Group theory requires that a linear term in the stress dependence must have opposite signs for $\Delta C_{44}$ and $\Delta C_{66}$, the latter with twice the slope of the former—the pure uniaxial stress $X$ along [001] belongs to the $(x^2+y^2-2z^2)$ row of the $\Gamma_{12}$ representation, and therefore contributions to the free energy [Eq. (1)] linear in $X$ and quadratic in the phonon displacements $\rho_{xy}$, $\rho_{yz}$, $\rho_{zx}$, must have the form

$$\delta F \propto (\rho_{xz}^2+\rho_{yz}^2-2\rho_{xy}^2)X \ . \tag{5}$$

This expression shows that the effect of stress on the singlet phonon, $\rho_{xy}$, has a slope of opposite sign and twice as large as that of the doublet, $\rho_{yz}$ and $\rho_{xz}$. This is borne out experimentally. From Fig. 3 we find the ratios $[\Delta C_{66}(X)-\Delta C_{66}(0)]/[\Delta C_{44}(X)-\Delta C_{44}(0)]$ in the range $-2.0$ to $-3.0$, always with $|\Delta C_{44}|$ increasing, and $|\Delta C_{66}|$ decreasing initially with increasing compression.

Now we turn the attention to the opposite limit: that of very high stresses. In Appendix A we have written the $6\times6$ $\vec{k}\cdot\vec{p}$ Hamiltonian relevant for the present band structure.[17,18] By assuming that the energy shifts produced by the external stress are large compared to typical band energies within the Fermi sea and also compared to the spin-orbit splitting $\Delta_0$, the secular equation can be solved by straightforward perturbation methods. We write the $6\times6$ Hamiltonian as follows:

$$H = H_0 + H' \tag{6}$$

with

$$H_0 = \begin{pmatrix} -F & 0 & 0 & 0 & 0 & 0 \\ 0 & F & -\sqrt{2}F & 0 & 0 & 0 \\ 0 & -\sqrt{2}F & -\Delta_0 & 0 & 0 & 0 \\ 0 & 0 & 0 & -\Delta_0 & \sqrt{2}F & 0 \\ 0 & 0 & 0 & \sqrt{2}F & F & 0 \\ 0 & 0 & 0 & 0 & 0 & -F \end{pmatrix}, \tag{7}$$

$$F = -3b\epsilon, \quad \epsilon = X/3(C_{11}-C_{12}) \ .$$

$\epsilon$ is here the traceless part of the strain associated with the uniaxial stress $X$, and it has the tensorial form

$$\overleftrightarrow{\epsilon} = \epsilon \begin{pmatrix} 1 & 0 & 0 \\ 0 & 1 & 0 \\ 0 & 0 & -2 \end{pmatrix} \ . \tag{8}$$

$b$ is a deformation potential constant, and $C_{11}$, $C_{12}$ are elastic stiffness constants.

Diagonalization of the Hamiltonian $H_0$ leads to the following set of zone-center eigenvalues:

$$\begin{aligned} \lambda_{l.h.} &= -F, \\ \lambda_{h.h.} &= \tfrac{1}{2}(F-\Delta_0)+\tfrac{1}{2}(9F^2+2F\Delta_0+\Delta_0^2)^{1/2}, \\ \lambda_{s.o.} &= \tfrac{1}{2}(F-\Delta_0)-\tfrac{1}{2}(9F^2+2F\Delta_0+\Delta_0^2)^{1/2} . \end{aligned} \tag{9}$$

The stress mixes the wave functions in the following manner [written on $(J, M_J)$ basis, see Appendix A]:

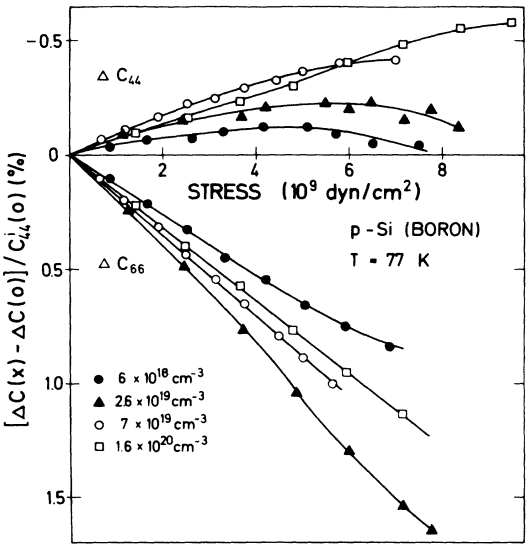


FIG. 3. Stress dependence of $\Delta C_{44}$ and $\Delta C_{66}$ for [001] uniaxial stress in $p$-Si samples of different impurity concentrations. The experimental temperature was 77 K.

$$
\begin{aligned}
&\psi^1_{\text{l.h.}} = \left|\tfrac{3}{2},\ \tfrac{3}{2}\right\rangle,\quad \psi^2_{\text{l.h.}} = \left|\tfrac{3}{2},\ -\tfrac{3}{2}\right\rangle,\\
&\psi^1_{\text{h.h.}} = a\left|\tfrac{3}{2},\ \tfrac{1}{2}\right\rangle + c\left|\tfrac{1}{2},\ \tfrac{1}{2}\right\rangle,\\
&\psi^2_{\text{h.h.}} = a\left|\tfrac{3}{2},\ -\tfrac{1}{2}\right\rangle - c\left|\tfrac{1}{2},\ -\tfrac{1}{2}\right\rangle,\\
&\psi^1_{\text{s.o.}} = -c\left|\tfrac{3}{2},\ \tfrac{1}{2}\right\rangle + a\left|\tfrac{1}{2},\ \tfrac{1}{2}\right\rangle,\\
&\psi^2_{\text{s.o.}} = c\left|\tfrac{3}{2},\ -\tfrac{1}{2}\right\rangle + a\left|\tfrac{1}{2},\ -\tfrac{1}{2}\right\rangle,
\end{aligned}
\tag{10}
$$

where

$$
\begin{aligned}
a &= \frac{1}{\sqrt{2}}\left(1+\frac{F+\Delta_0}{(9F^2+2F\Delta_0+\Delta_0^2)^{1/2}}\right)^{1/2},\\
c &= -\frac{1}{\sqrt{2}}\left(1-\frac{F+\Delta_0}{(9F^2+2F\Delta_0+\Delta_0^2)^{1/2}}\right)^{1/2}.
\end{aligned}
\tag{11}
$$

On the original $(J, M_J)$ basis the perturbation Hamiltonian $H'$ has the following form:

$$
H' = \begin{pmatrix}
0 & Q & -Q/\sqrt{2} & -\sqrt{2}G & G & 0\\
Q^* & 0 & 0 & \sqrt{\tfrac{3}{2}}Q & 0 & G\\
-Q^*/\sqrt{2} & 0 & 0 & 0 & \sqrt{\tfrac{3}{2}}Q & \sqrt{2}G\\
-\sqrt{2}G^* & \sqrt{\tfrac{3}{2}}Q^* & 0 & 0 & 0 & -Q/\sqrt{2}\\
G^* & 0 & \sqrt{\tfrac{3}{2}}Q^* & 0 & 0 & Q\\
0 & G^* & \sqrt{2}\,G^* & -Q^*/\sqrt{2} & -Q^* & 0
\end{pmatrix},
\tag{12}
$$

where for a general $\vec{k}$ vector, and an acoustical phonon $(\rho_{xy},\ \rho_{xz},\ \rho_{yz})$,

$$
\begin{aligned}
Q &= -\left[d\rho_{xz} + Bk_xk_z - i(d\rho_{yz} + Bk_yk_z)\right],\\
G &= -\tfrac{1}{2}\sqrt{3}\,B(k_x^2-k_y^2) + i(d\rho_{xy} + Dk_xk_y).
\end{aligned}
\tag{13}
$$

At high stresses, all the carriers will be in h. h., which therefore is the only band of interest. To second order in perturbation theory, the energy of h. h. becomes

$$
E_{\text{h.h.}} = \lambda_{\text{h.h.}} + \sum_j{}' \frac{|H_{(\text{h.h.})j}|^2}{\lambda_{\text{h.h.}} - \lambda_j},
\tag{14}
$$

or

$$
\begin{aligned}
\delta E_{\text{h.h.}} &= E_{\text{h.h.}} - \lambda_{\text{h.h.}}\\
&= \frac{(a - c/\sqrt{2})^2|Q|^2 + (a + c\sqrt{2})^2|G|^2}{\tfrac{1}{2}(3F-\Delta_0) + \tfrac{1}{2}(9F^2+2F\Delta_0+\Delta_0^2)^{1/2}}\\
&\quad + \frac{3}{2}\,\frac{|Q|^2}{(9F^2+2F\Delta_0+\Delta_0^2)^{1/2}}.
\end{aligned}
\tag{15}
$$

Consider first the extreme-high-stress limit $F \gg \Delta_0$. In this case $a = \sqrt{\frac{2}{3}}$, $c = -\sqrt{\frac{1}{3}}$ leading to

$$
\begin{aligned}
\delta E_{\text{h.h.}} &= |Q|^2/F\\
&= -(1/3b\epsilon)\left[d^2(\rho_{xz}^2+\rho_{yz}^2) + B^2(k_x^2+k_y^2)k_z^2\right.\\
&\quad \left. + 2Bd(\rho_{xz}k_xk_z + \rho_{yz}k_yk_z)\right].
\end{aligned}
\tag{16}
$$

From this we obtain the contribution to the free energy from the leading term in $\epsilon$, according to Eq. (1):

$$
\begin{aligned}
\delta F &= \sum_k f_k\,\delta E_k^{(2)} + \frac{1}{2}\sum_k \frac{\partial f_k}{\partial E_k}(\delta E_k^{(1)})^2\\
&\simeq -\frac{Nd^2}{3b\epsilon}(\rho_{xz}^2+\rho_{yz}^2).
\end{aligned}
\tag{17}
$$

$N$ is the total number of free carriers per cm$^3$. By comparing with an equivalent expression for $\delta F$ written in terms of the tetragonal constants we find:

$$
\Delta C_{44} = -Nd^2/6b\epsilon,\quad \Delta C_{66} = 0.
\tag{18}
$$

Thus, we have shown that both $\Delta C_{44}$ and $\Delta C_{66}$ disappear at very large stresses: $\Delta C_{44}$ as $X^{-1}$, and $\Delta C_{66}$ as a higher power in $(1/X)$. It can easily be seen that by retaining the stress dependence in $a$ and $c$ [Eq. (11)], the leading term in the stress dependence of $\Delta C_{66}$ is proportional to $X^{-3}$.

Owing to the inavailability of high-stress data on the elastic constants, the asymptotic dependence of $C_{44}$ and $C_{66}$ calculated here cannot be directly tested. However, in the Raman experiment[13] (see following paper, II) such data can be obtained for low-concentration samples (see data on $6\times10^{18}$ cm$^{-3}$) essentially confirming the $X^{-1}$ behavior predicted for the doublet. Nonetheless, the discussion above leads to conclusions about the qualitative behavior of the stress dependences of $\Delta C_{44}$ and $\Delta C_{66}$ in agreement with experiment: By continuity, if $|\Delta C_{44}|$ were initially (for small stresses) to increase, and at high stresses to disappear, it must necessarily pass through a maximum. Such a behavior is indeed indicated in the experiments, particularly for the low-concentration samples (and very clearly confirmed in the Raman Experiments in II). If $\Delta C_{66}$ were to decrease initially, and then disappear, one would expect a monotonic decrease over the entire range of stresses. Again this is confirmed by the experiments.

In the opposite limit, that of small stresses, the calculation of he initial slope in $\Delta C_{66}$ and $\Delta C_{44}$ will be outlined. For certain details of the treatment we refer to Appendix B. We again divide the dis-

cussion into two parts: First, the problem is considered in the low-concentration limit, essentially extending the Bir and Tursunov theory,[8] to include a small external stress. Second, the high-concentration case is developed along the same lines.

The starting point in the low concentration limit is the Dresselhaus, Kip, and Kittel[17] expression for the parabolic region of h. h. (−) and l. h. (+) ($\Delta_0 \gg E_{\text{l.h.}}, E_{\text{h.h.}}$): Adapted to our situation their expression is [it can also be extracted from Eq. (A2) in Appendix A]

$$E(\epsilon, \rho) = Ak^2 \pm (E_k + E_{k\epsilon} + E_\epsilon + E_{k\rho} + E_\rho)^{1/2}, \quad (19)$$

where the upper (lower) sign refers to l. h. (h. h.). This convention is maintained throughout. Further

$$\text{static} \begin{cases} E_k = B^2k^4 + C^2(k_x^2k_y^2 + k_x^2k_z^2 + k_y^2k_z^2) \simeq \bar{B}^2k^4, \\ E_{k\epsilon} = 3Bb\epsilon(2k_z^2 - k_x^2 - k_y^2), \\ E_\epsilon = 9b^2\epsilon^2, \end{cases}$$

$$\lambda = E(\epsilon, 0) = (E_k + E_{k\epsilon} + E_\epsilon)^{1/2}, \quad (20)$$

$$\text{ultra-sound} \begin{cases} E_{k\rho} = 2dD(\rho_{xy}k_xk_y + \rho_{xz}k_xk_z + \rho_{yz}k_yk_z), \\ E_\rho = d^2(\rho_{xy}^2 + \rho_{xz}^2 + \rho_{yz}^2). \end{cases}$$

(Note $A$, $B$, $\bar{B}$, $b$, $d$, and $\epsilon$ are *negative* in absolute sign.) The energy shift due to the ultrasonic strain is:

$$\delta E(\epsilon, \rho) = E(\epsilon, \rho) - E(\epsilon, 0). \quad (21)$$

By expanding $\delta E(\epsilon, \rho)$ to second order in $\rho$ we obtain, in agreement with previous notation,

$$\delta E^{(1)} = \pm \frac{1}{2}\frac{E_{k\rho}}{\lambda}, \qquad \delta E^{(2)} = \pm \frac{1}{2\lambda}\left(E_\rho - \frac{1}{4}\frac{E_{k\rho}^2}{\lambda^2}\right). \quad (22)$$

$(\delta E^{(1)})^2$ is expanded to first power in the uniaxial strain and averaged over all directions in $k$ space (see Appendix B), leading to

$$\langle(\delta E^{(1)})^2\rangle = \frac{d^2D^2}{15\bar{B}^2}\left((\rho_{xy}^2 + \rho_{xz}^2 + \rho_{yz}^2) + \frac{6Bb\epsilon}{7\bar{B}^2k^2}(2\rho_{xy}^2 - \rho_{xz}^2 - \rho_{yz}^2)\right) \quad (23)$$

This gives the following contribution to the free energy [second term in Eq. (1)]:

$$\begin{aligned}\delta F^{(1)} &= \frac{1}{2}\sum_k \frac{\partial f_k}{\partial E_k}\langle(\delta E^{(1)})^2\rangle \\ &= -\frac{2\pi}{15h^3}\frac{d^2D^2}{\bar{B}^2}[(2m_H)^{3/2} + (2m_L)^{3/2}]|\mu|^{1/2} \\ &\quad\times(\rho_{xy}^2 + \rho_{xz}^2 + \rho_{yz}^2) \\ &\quad - \frac{1}{35\pi}\frac{d^2D^2Bb\epsilon}{h\bar{B}^4}[(2m_H)^{1/2} + (2m_L)^{1/2}]|\mu|^{-1/2} \\ &\quad\times(2\rho_{xy}^2 - \rho_{xz}^2 - \rho_{yz}^2). \end{aligned} \quad (24)$$

When considering the free-energy term associated with $\delta E^{(2)}$, special caution is required: A difficulty arises when $\lambda$ in Eq. (21) is expanded to first power in $\epsilon$. Such an expansion leads to a divergence in the term linear in $\epsilon$, when the sum over occupied states is performed. As shown in Appendix B, this difficulty is avoided by deferring the expansion in $\epsilon$ until after the $\vec{k}$-space summation. In practical terms this is equivalent to neglecting the contribution arising from the lower limit of integration when converting $\sum_k \to \int_0^\mu dE\, g(E)$. With this in mind $\lambda$ in Eq. (21) can be expanded to first order in $\epsilon$, as before, yielding for the angular average of $\delta E^{(2)}$

$$\begin{aligned}\langle\delta E^{(2)}\rangle &= \pm\frac{d^2}{2k^2}\left(1 - \frac{1}{15}\frac{D^2}{\bar{B}^2}\right)(\rho_{xy}^2 + \rho_{xz}^2 + \rho_{yz}^2) \\ &\quad \mp \frac{3}{70}\frac{d^2D^2Bb\epsilon}{\bar{B}^5k^4}(2\rho_{xy}^2 - \rho_{xz}^2 - \rho_{yz}^2), \end{aligned} \quad (25)$$

and for $\delta F^{(2)}$

$$\begin{aligned}\delta F^{(2)} &= \sum_k f_k\langle\delta E^{(2)}\rangle \\ &= -\frac{1}{\pi}\frac{d^2}{\bar{B}h}\left(1 - \frac{D^2}{15\bar{B}^2}\right) \\ &\quad\times[(2m_H)^{1/2} - (2m_L)^{1/2}]|\mu|^{1/2}\times(\rho_{xy}^2 + \rho_{xz}^2 + \rho_{yz}^2) \\ &\quad + \frac{3\hbar^2}{70\pi h}\frac{d^2D^2Bb\epsilon}{\bar{B}^5(m_Lm_H)^{1/2}}[(2m_H)^{1/2} - (2m_L)^{1/2}] \\ &\quad\times|\mu|^{-1/2}(2\rho_{xy}^2 - \rho_{xz}^2 - \rho_{yz}^2). \end{aligned} \quad (26)$$

The terms symmetric in $\rho_{xy}^2$, $\rho_{xz}^2$, and $\rho_{yz}^2$ of Eqs. (24) and (26) give the low-temperature limit of the Bir and Tursunov formula, from which Eq. (3) can be obtained by including the proper temperature dependence (see Refs. 1 and 2). Here we are interested in the free-energy term linear in $\epsilon$. By adding the contributions from $\delta F^{(1)}$ and $\delta F^{(2)}$ and comparing with the free-energy expression in terms of the tetragonal elastic constants, we obtain

$$\begin{aligned}\Delta C'_{66} &= -\frac{3}{105\pi}\frac{d^2D^2Bb\epsilon}{h\bar{B}^4}\left((2m_H)^{1/2} + (2m_L)^{1/2}\right. \\ &\quad\left. - \frac{3\hbar^2}{2\bar{B}(m_Lm_H)^{1/2}}[(2m_H)^{1/2} - (2m_L)^{1/2}]\right)|\mu|^{-1/2}, \\ \Delta C'_{44} &= -\tfrac{1}{2}\Delta C'_{66}. \end{aligned} \quad (27)$$

We note that these expressions are, necessarily, in agreement with the group-theoretical argument presented earlier. Furthermore (since $B$, $\bar{B}$, $b$, and $\epsilon$ are negative), $\Delta C'_{66}$ is positive, i.e., $|\Delta C_{66}|$ is reduced with stress, in accordance with the experiments.

We use the following values for the various numerical constants: $d = -4.85$ eV, $b = -2.1$ eV,[19]

$B = -0.75\hbar^2/2m_0$, $C^2 = 27.56(\hbar^2/2m_0)^2$, $\bar{B}^2 = B^2 + \frac{1}{5}C^2 = 6.075(\hbar^2/2m_0)^2$, $m_H = 0.5m_0$, $m_L = 0.16m_0$,[20] $C_{44} = 0.976\times10^{12}$ dyn/cm$^2$, $(C_{11}-C_{12}) = 1.026\times10^{12}$ dyn/cm$^2$ (at 77 K).[5] We thereby obtain the following value for the initial (low-stress) slope of $\Delta C_{66}$ versus stress:

$$\frac{\Delta C'_{66}/C^i_{44}}{X\,(\text{kbar})} = 1.34\times10^{-4}\,|\mu(\text{eV})|^{-1/2}\,. \tag{28}$$

This slope has been computed for the samples used and is compared with the experimental slopes in Table II.

As expected the slope deviates from the predicted value when the Fermi level is of the order of the spin-orbit splitting or larger. ($N = 2.6\times10^{19}$ cm$^{-3}$ or higher). However, for the lowest-concentration sample ($N = 6\times10^{18}$ cm$^{-3}$) the Bir and Tursunov condition ($\mu \ll \Delta_0$) is approximately satisfied, and as a consequence the theory reproduces the experimental value to within about 30%. This agreement must be considered as very satisfactory in view of the complicated band structure at hand and the accumulating uncertainties in the parameters used for the theoretical evaluation.

In an attempt to fit the slopes for the high-concentration samples we return to a band model described earlier, assuming h. h. and l. h. being parabolic (both with a h. h. mass) and running parallel with a separation of $\frac{2}{3}\Delta_0$. Again s. o. is neglected. The procedure for this case is to consider the bands along the three- and fourfold axes when applying stress. The additional energy shifts under the action of the ultrasonic strain ($\rho_{xy}$, $\rho_{xz}$, $\rho_{yz}$) are then computed and the angular averages $\langle(\delta E^{(1)})^2\rangle$ and $\langle\delta E^{(2)}\rangle$ are calculated. In this case, however, the angular average is approximated by the weighted average for all the $\langle100\rangle$ and the $\langle111\rangle$ directions.

For the purpose of this calculation it is useful to choose the axis of quantization ($\bar{z}$ axis) parallel to $\vec{k}$. The $\bar{x}$ axis is chosen to be along the direction $\hat{n}\times\vec{k}$ ($\hat{n}$ is a unit vector along the stress axis, i.e., [001]), and the $\bar{y}$ axis to be parallel to $\bar{z}\times\bar{x}$.

The wave functions for this case have the following form[18]:

$$\begin{aligned} |v_1\rangle &= -\frac{1}{\sqrt{2}}(\bar{x}+i\bar{y})\uparrow, \quad |v_3\rangle = \frac{1}{\sqrt{2}}(\bar{x}-i\bar{y})\downarrow, \\ |v_2\rangle &= \frac{1}{\sqrt{2}}(\bar{x}-i\bar{y})\uparrow, \quad |v_4\rangle = -\frac{1}{\sqrt{2}}(\bar{x}+i\bar{y})\downarrow, \end{aligned} \tag{29}$$

where $\uparrow$ and $\downarrow$ indicate spin up and spin down, respectively. The matrix elements of the electron-phonon interaction Hamiltonian (see Appendix A) are for any given direction of $\vec{k}$

$$\begin{aligned} \langle v_{1(2)}|H_{ep}|v_{1(2)}\rangle &= \tfrac{1}{2}(\langle\bar{x}|H_{ep}|\bar{x}\rangle + \langle\bar{y}|H_{ep}|\bar{y}\rangle), \\ \langle v_{1(2)}|H_{ep}|v_{2(1)}\rangle &= -\tfrac{1}{2}(\langle\bar{x}|H_{ep}|\bar{x}\rangle - \langle\bar{y}|H_{ep}|\bar{y}\rangle) \\ &\quad \pm i\langle\bar{x}|H_{ep}|\bar{y}\rangle\,. \end{aligned} \tag{30}$$

The resulting $2\times2$ secular determinant has the solution

$$E = \langle v_1|H_{ep}|v_1\rangle \pm (\lambda^2 + |\langle v_1|H_{ep}|v_2\rangle|^2)^{1/2}\,. \tag{31}$$

Note that here + refers to l. h., while − refers to h. h. $E$ is found for a given stress, $E(\epsilon, 0)$; and for stress *and* ultrasonic strain, $E(\epsilon, \rho)$. The shift due to the ultrasonic strain is that expanded to include first order $\delta E^{(1)}$ and second order $\delta E^{(2)}$ in $\rho$, as before. The resulting angular averages of $(\delta E^{(1)})^2$ and $\delta E^{(2)}$ are to first order in $\epsilon$ (for details, see Appendix B):

$$\langle(\delta E^{(1)})^2\rangle = \frac{4}{21}d^2(\rho_{xy}^2+\rho_{xz}^2+\rho_{yz}^2) \pm \frac{24}{7}\frac{b\epsilon}{\Delta_0}d^2(2\rho_{xy}^2-\rho_{xz}^2-\rho_{yz}^2)\,, \tag{32}$$

$$\langle\delta E^{(2)}\rangle = \pm\frac{25}{14}\frac{d^2}{\Delta_0}(\rho_{xy}^2+\rho_{xz}^2+\rho_{yz}^2)\,. \tag{33}$$

The contribution to the free energy [Eq. (1)] is, in this case, evaluated for a degenerate electron gas ($T = 0$ K):

TABLE II. $\Delta C'_{66}/C^i_{44}$ versus $X$ in the limit of small stresses. The experimental values are compared with estimates from the expressions derived for the low-concentration limit (LC) and for the high-concentration limit (HC). $T = 77$ K.

| Sample ($10^{19}$ cm$^{-3}$) | 0.6 | 2.6 | 7 | 16 |
|---|---|---|---|---|
| $\lvert\mu\rvert$ (meV) | 17 | 40 | 69 | 114 |
| $\left(\frac{\Delta C'_{66}/C^i_{44}}{X}\right)_{EXP}$ (% kbar$^{-1}$) | 0.130 | 0.198 | 0.173 | 0.155 |
| $\left(\frac{\Delta C'_{66}/C^i_{44}}{X}\right)_{LC}$ (% kbar$^{-1}$) | 0.103 | 0.067 | 0.051 | 0.040 |
| $\left(\frac{\Delta C'_{66}/C^i_{44}}{X}\right)_{HC}$ (% kbar$^{-1}$) | ... | 0.030 | 0.020 | 0.014 |

$$\delta F = -\frac{d^2}{42}\left(\frac{75}{\Delta_0}(N_H - N_L) + 4(g_H + g_L)\right)(\rho_{xy}^2 + \rho_{xz}^2 + \rho_{yz}^2)$$
$$+ \frac{12}{7}\frac{b\epsilon}{\Delta_0} d^2(g_H - g_L)(2\rho_{xy}^2 - \rho_{xz}^2 - \rho_{yz}^2) . \quad (34)$$

$N_H$ and $N_L$ are the total number of carriers in h. h. and l. h., respectively. $g_H$ and $g_L$ are the densities of states at the Fermi surface in the respective bands.

Again the term symmetric in $\rho_{xy}^2$, $\rho_{xz}^2$, and $\rho_{yz}^2$ gives the low-temperature limit of the zero-stress contribution to $\Delta C_{44}$, and can be cast into the form shown in Eq. (4) (see Appendix B). From Eq. (34) we can now obtain the lowest-order stress dependence in $\Delta C_{66}$ and $\Delta C_{44}$:

$$\Delta C'_{66} = \frac{12}{7}\frac{b\epsilon}{\Delta_0} d^2(g_H - g_L) ,$$
$$\Delta C'_{44} = -\tfrac{1}{2}\Delta C'_{66} . \quad (35)$$

We again note that the group-theoretical requirement ($\Delta C'_{44} = -\frac{1}{2}\Delta C'_{66}$) is satisfied.

The values of the slope $(\Delta C'_{66}/C^i_{44})/X$ have been calculated for the relevant impurity concentrations and are shown in Table II. By comparison with the experimental data, we observe that this calculation results in an underestimation of the measured slopes by an order of magnitude. The most likely explanation for this discrepancy is that we are not sampling a representative set of directions in $\vec{k}$ space for our angular average of the *stress behavior*, indicating one limitation of the simple high-concentration limit used here. The same difficulty did not occur for the Bir-Tursunov limit, where the angular average is a more realistic one.

Finally in this section, we would like to draw the attention to a particular property of the stress data. We have noted that experimentally $|\Delta C_{66}|$ decreases nearly linearly with stress over the entire range of stresses used. The slope should flatten out at large stress, as $\Delta C_{66}$ approaches zero. This decrease in slope is observed for the $6\times10^{18}$-cm$^{-3}$ sample in Fig. 3 but not for the other samples, owing to the limited range of stresses at hand in this experiment. However, for the Raman singlet (see II) the same behavior is also evident for higher-concentration samples. The curious fact in all these cases is that $\Delta C_{66}$ (and the carrier effect on the Raman singlet) extrapolates to zero for a stress $X$, corresponding to l. h. passing through the Fermi surface. In Table III we show a comparison of the extrapolated stress $X_2$ (where $|\Delta C_{66}| = 0$) and the calculated stress $X_1$ [when $|E_{\text{h.h.}} - E_{\text{l.h.}}| = \mu(X_1)$].

The condition $\Delta C_{66} = 0$ is satisfied when the (extrapolated) stress induced change in $\Delta C_{66}$ equals the total shift $\Delta C_{44}$ discussed in Sec. II. Note that $\Delta C_{44}$ was measured at 300 K, but can easily be converted to 77 K (listed in Table III) from the temperature dependence in Eq. (4).

TABLE III. Comparison of stress for which l. h. passes through the Fermi level, with extrapolated stress for which $\Delta C_{66} = 0$. The table also shows Fermi level versus impurity content with all carriers in h. h., and $\Delta C_{44}/C^i_{44}$ $(X = 0)$ for $T = 77$ K.

| Sample ($10^{19}$ cm$^{-3}$) | 0.6 | 2.6 | 7 | 16 |
|---|---|---|---|---|
| $\lvert\mu(X_1)\rvert$ (meV) for all carriers in h. h. | 24 | 64 | 124 | 215 |
| Stress $X_1$ (kbar) where $E_{\text{h.h.}} - E_{\text{l.h.}} = \mu$ | 5.0 | 12.0 | 22.0 | 36.8 |
| Stress $X_2$ (kbar) where $\Delta C_{66} = 0$ (extrapol.) | 4.5 | 11.0 | 20.6 | 30.9 |
| $\Delta C_{44}/C^i_{44}$ (%) at 77 K | −0.58 | −1.95 | −3.31 | −4.94 |

The strong correlation between the stresses $X_1$ and $X_2$ in Table III suggests that an *inter*band redistribution mechanism dominates the behavior of $\Delta C_{66}$, i.e., $\Delta C_{66}$ vanishes when l. h. is moved out of the Fermi sea. On the other hand $\Delta C_{44}$ should be dominated by *intra*band redistribution, since $|\Delta C_{44}|$ has its maximum value where l. h. passes through the Fermi level. We recall the earlier conclusion that $\Delta C_{66} \propto X^{-3}$ for high stresses where only interband redistribution is possible; while $\Delta C_{44} \propto X^{-1}$, lending credence to the above observation.

As for the linear stress dependence of $\Delta C_{66}$, we can only argue that this is consistent with the fact that the observed slope does not change appreciably from sample to sample: The slope is insensitive to the Fermi energy, and is not influenced by this as it changes with stress [one can appreciate the change in $\mu$ by comparing the values in Table I, $\mu(X = 0)$, with those in Table III, $\mu(X = X_1)$].

## IV. CONCLUSIONS

In this paper we have presented the results of a systematic investigation of the effect of free carriers on the elastic constant $C_{44}$ in $p$-Si. We measured the concentration dependence of $\Delta C_{44}$ and compared it with simple band-model calculations in the low- and high-concentration limit. As one measure of the free-carrier effect in $\Delta C_{44}$ we defined the band parameter $K(\mu)$, which could be calculated in those two limits; and the values found were in satisfactory agreement with those obtained experimentally.

By applying a strong uniaxial stress to the samples, the free-carrier effects to $C_{44}$ are expected to disappear. We could not see this, except possibly for $\Delta C_{66}$ in the $6\times10^{18}$-cm$^{-3}$ sample, owing to the limited stress range that could be applied.

However, we have developed theories for the low- and high-stress limits, predicting qualitative features of $\Delta C_{44}$ versus stress in agreement with the observations. A quantitative estimate for the low-stress low-concentration case proved to be in very good agreement with the experimental data for the $6\times10^{18}$-cm$^{-3}$ sample. A similar estimate for the high-concentration case was off by an order of magnitude, a fact that can be attributed to inadequacies in the model.

In conclusion, we can state that semiquantitative, and in some cases quantitative, confirmation of the Keyes mechanism for the free-carrier effects on the elastic constant $C_{44}$ in $p$-Si has been achieved. The experimental data were compared to various calculations based on models for the valence bands, yielding information as to the applicability of such models in calculations of this nature.

## APPENDIX A

The band calculations performed in this work are based on the combined strain kinetic energy Hamiltonian[11,18]

$$H = \mathfrak{A}\,\mathrm{Tr}(\overleftrightarrow{\alpha}) - 3\mathfrak{B}[(L_x^2 - \tfrac{1}{3}L^2)\,\alpha_{xx} + \text{c. p.}] - 3\sqrt{3}\,\mathfrak{D}[\{L_xL_y\}\,\alpha_{xy} + \text{c. p.}]\ , \quad \text{(A1)}$$

c.p. means cyclic permutation. $\overleftrightarrow{\alpha}$ is any symmetric tensor (either strain $\epsilon_{ij}$ or $k$-vector combinations $k_ik_j$); $\{L_iL_j\}$ means $\frac{1}{2}(L_iL_j + L_jL_i)$; $\mathfrak{A}$, $\mathfrak{B}$, and $\mathfrak{D}$ are the appropriate deformation potentials or band parameter constants. On a $(J, M_J)$ basis ($J = \frac{3}{2}$), (A1) can be written as a $6\times6$ matrix of the following form[18]:

$$H = \begin{pmatrix} -F & Q & -Q/\sqrt{2} & -\sqrt{2}G & G & 0 \\ Q^* & F & -\sqrt{2}F & \sqrt{\frac{3}{2}}Q & 0 & G \\ -Q^*/\sqrt{2} & -\sqrt{2}F & -\Delta_0 & 0 & \sqrt{\frac{3}{2}}Q & \sqrt{2}G \\ -\sqrt{2}G^* & \sqrt{\frac{3}{2}}Q^* & 0 & -\Delta_0 & \sqrt{2}F & -Q/\sqrt{2} \\ G^* & 0 & \sqrt{\frac{3}{2}}Q^* & \sqrt{2}F & F & -Q \\ 0 & G^* & \sqrt{2}G^* & -Q^*/\sqrt{2} & -Q^* & -F \end{pmatrix}\ , \quad \text{(A2)}$$

where the columns correspond to $|\frac{3}{2}, \frac{3}{2}\rangle$, $|\frac{3}{2}, \frac{1}{2}\rangle$, $|\frac{1}{2}, \frac{1}{2}\rangle$, $|\frac{1}{2}, -\frac{1}{2}\rangle$, $|\frac{3}{2}, -\frac{1}{2}\rangle$, and $|\frac{3}{2}, -\frac{3}{2}\rangle$, respectively. The term $\mathfrak{A}\mathrm{Tr}(\overleftrightarrow{\alpha})$ in Eq. (A1) provides a uniform energy shift of all states and has been omitted in Eq. (A2), but can be added at the end. The different terms in Eq. (A2) are given by

$$F = \tfrac{1}{2}\mathfrak{B}(2\alpha_{zz} - \alpha_{xx} - \alpha_{yy})\ ,$$
$$G = -\tfrac{1}{2}\sqrt{3}\,\mathfrak{B}(\alpha_{xx} - \alpha_{yy}) + i\,\mathfrak{D}\alpha_{xy}\ , \quad \text{(A3)}$$
$$Q = -\mathfrak{D}(\alpha_{xz} - i\alpha_{yz})\ ,$$

with

$$\alpha_{ij} = b\epsilon_{ij} + B k_i k_j\ , \quad \mathfrak{B} = 1 \quad (i = j)$$
$$= d\epsilon_{ij} + D k_i k_j\ , \quad \mathfrak{D} = 1 \quad (i \neq j). \quad \text{(A4)}$$

For the purpose of computing the Fermi energy versus carrier concentration and versus stress we diagonalized the $6\times6$ Hamiltonian [Eq. (A2)] for all fourfold, threefold, and twofold directions in $\vec{k}$ space and used a weighted average of the resulting bands. These average bands for zero external stress are shown in Fig. 4.

The Fermi level versus carrier contents (for any given stress) is determined by the relationship

$$N = \frac{2}{(2\pi)^3}\,\frac{4\pi}{3}\,(k^3_{\text{h.h.}} + k^3_{\text{l.h.}} + k^3_{\text{s.o.}})\ , \quad \text{(A5)}$$

where $k_{\text{h.h.}}$, $k_{\text{l.h.}}$, and $k_{\text{s.o.}}$ are the Fermi level intersects with the average bands. The zero-stress and high-stress values of $\mu$ versus $N$ are shown in Fig. 1 (Sec. I).

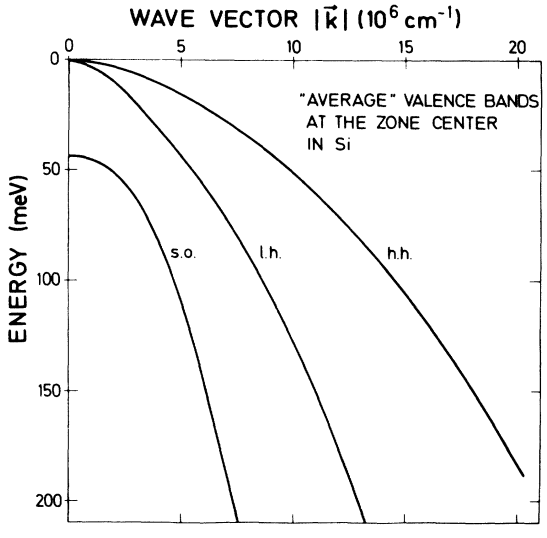


FIG. 4. Valence bands in Si as weighted average of bonds for all ⟨100⟩, ⟨111⟩, and ⟨110⟩ directions (zero stress).

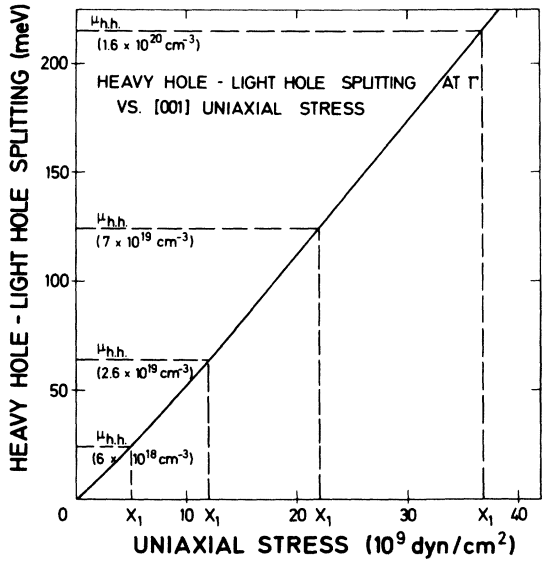


FIG. 5. h. h. -l. h. splitting vs [001] uniaxial stress. The horizontal lines represent high stress values of Fermi levels [$\mu_{h.h.} = \mu(X_1)$] for various carrier contents. The intersects with the curve shows the stresses for which l. h. passes through the Fermi surface.

In Fig. 5 is shown the h. h. -l. h. splitting with stress at the zone center, used for determining when the top of l. h. passes through the Fermi surface.

## APPENDIX B

For the purpose of computing the initial slopes in $\Delta C_{44}$ and $\Delta C_{66}$ versus stress in the low-concentration limit, we start with the expressions (19) to (22) in Sec. III. In order to find the contribution to the free energy through redistribution we have to calculate the angular averages of the following quantities:

$$(\delta E^{(1)})^2 = dD^2 \frac{\rho_{xy}^2 k_x^2 k_y^2 + \rho_{xz}^2 k_x^2 k_z^2 + \rho_{yz}^2 k_y^2 k_z^2}{\bar{B}^2 k^4 + 3bB\epsilon(2k_z^2 - k_x^2 - k_y^2) + 9b^2\epsilon^2} , \tag{B1}$$

$$\delta E^{(2)} = \pm \frac{d^2}{2} \frac{\rho_{xy}^2 + \rho_{xz}^2 + \rho_{yz}^2}{[\bar{B}^2 k^4 + 3bB\epsilon(2k_z^2 - k_x^2 - k_y^2) + 9b^2\epsilon^2]^{1/2}} \mp \frac{d^2 D^2}{2} \frac{\rho_{xy}^2 k_x^2 k_y^2 + \rho_{xz}^2 k_x^2 k_z^2 + \rho_{yz}^2 k_y^2 k_z^2}{[\bar{B}^2 k^4 + 3bB\epsilon(2k_z^2 - k_x^2 - k_y^2) + 9b^2\epsilon^2]^{3/2}} . \tag{B2}$$

In Eq. (B1) and in the first term in (B2) we can expand to first order in $\epsilon$ without causing difficulties when performing the $\vec{k}$ summation in Eq. (1). By using the following angular averages, the expression (21) and part of Eq. (23) can be obtained:

$$\begin{aligned} &\langle k_x^2 k_y^2 (2k_z^2 - k_x^2 - k_y^2)\rangle = -\tfrac{4}{105} k^6 , \\ &\langle k_x^2 k_z^2 (2k_z^2 - k_x^2 - k_y^2)\rangle = \tfrac{2}{105} k^6 , \\ &\langle k_y^2 k_z^2 (2k_z^2 - k_x^2 - k_y^2)\rangle = \tfrac{2}{105} k^6 , \\ &\langle k_x^2 k_y^2\rangle = \langle k_x^2 k_z^2\rangle = \langle k_y^2 k_z^2\rangle = \tfrac{1}{15} k^4 . \end{aligned} \tag{B3}$$

In order to calculate the last term in Eq. (B2) (hereafter referred to as $\delta E^{(2)\prime}$), we defer the expansion in $\epsilon$ until later and use a weighted average of all [100], [111], and [110] directions as an angular average:

$$\langle \delta E^{(2)\prime} \rangle = \mp \frac{dD^2}{104} \left( \frac{k^4(\rho_{xz}^2 + \rho_{yz}^2)}{(\bar{B}^2 k^4 + \frac{3}{2} Bk^2 b\epsilon + 9b^2\epsilon^2)^{3/2}} + \frac{k^4 \rho_{xy}}{(\bar{B}^2 k^4 - 3Bk^2 b\epsilon + 9b^2\epsilon^2)^{3/2}} \right) . \tag{B4}$$

This corresponds to the free-energy contribution:

$$\delta F^{(2)\prime} = \sum_k f_k \langle \delta E^{(2)\prime} \rangle . \tag{B5}$$

The summation over $k$ leads to the following type of integration in energy:

$$I \propto \int_0^\mu dE \frac{E^{5/2}}{(E^2 + a\epsilon E + \epsilon^2)^{3/2}} . \tag{B6}$$

This integral has no obvious analytic solution, but since the integrand has the form $E^{5/2}$ for $E \ll a\epsilon$, the contribution from the lower limit of integration disappears. For $\mu \gg a\epsilon$, we can therefore safely expand the integrand to first order in $\epsilon$ and perform the integration, retaining only the contribution from the upper limit of integration. This therefore justifies the procedure used in Eq. (25) and (26) of the main text.

In the high-concentration limit we have to consider the matrix elements of Eq. (30) in the following nonequivalent directions (when both uniaxial and ultrasonic strains are present):

| | | | |
|---|---|---|---|
| $\hat{k} \parallel [001]$: | $\bar{x} = x$, | $\bar{y} = y$, | $\bar{z} = z$, |
| $\hat{k} \parallel [100]$: | $\bar{x} = y$, | $\bar{y} = z$, | $\bar{z} = x$, |
| $\hat{k} \parallel [010]$: | $\bar{x} = -x$, | $\bar{y} = z$, | $\bar{z} = y$, |
| $\hat{k} \parallel [111]$: | $\bar{x} = \frac{1}{\sqrt{2}}(-x+y)$, | $\bar{y} = -\frac{1}{\sqrt{6}}(x+y) + \sqrt{\frac{2}{3}} z$, | $\bar{z} = \frac{1}{\sqrt{3}}(x+y+z)$, |

$$\hat{k} \parallel [\bar{1}11]: \quad \bar{x} = -\frac{1}{\sqrt{2}}(x+y), \quad \bar{y} = \frac{1}{\sqrt{6}}(x-y)+\sqrt{\tfrac{2}{3}}z, \quad \bar{z} = \frac{1}{\sqrt{3}}(-x+y+z),$$

$$\hat{k} \parallel [1\bar{1}1]: \quad \bar{x} = \frac{1}{\sqrt{2}}(x+y), \quad \bar{y} = -\frac{1}{\sqrt{6}}(x-y)+\sqrt{\tfrac{2}{3}}z, \quad \bar{z} = \frac{1}{\sqrt{3}}(x-y+z), \tag{B7}$$

$$\hat{k} \parallel [\bar{1}\bar{1}1]: \quad \bar{x} = \frac{1}{\sqrt{2}}(x-y), \quad \bar{y} = \frac{1}{\sqrt{6}}(x+y)+\sqrt{\tfrac{2}{3}}z, \quad \bar{z} = \frac{1}{\sqrt{3}}(-x-y+z).$$

The following matrix elements are being used[18]:

$$\langle x|H_{ep}|x\rangle = \langle y|H_{ep}|y\rangle = -3b\epsilon\,,$$

$$\langle z|H_{ep}|z\rangle = 6b\epsilon\,, \tag{B8}$$

$$\langle x|H_{ep}|y\rangle = \sqrt{3}d\rho_{xy} \text{ and c.p. .}$$

Using (B7) and (B8) in conjunction with Eq. (31) the "angular averages" of Eq. (32) and Eq. (33) are obtained.

From the final expression [Eq. (34)] of the free-energy contribution, we can extract the low-temperature limit of the zero-stress value of $\Delta C_{44}$:

$$\Delta C_{44} = -\frac{d^2}{84}\left(\frac{75}{\Delta_0}(N_H - N_L) + 4(g_H + g_L)\right)\,. \tag{B9}$$

Equation (B9) can be expressed in terms of the total number of carriers along the same lines as used in Ref. 11. The first term is exactly the same as the one obtained in that reference, while the second term represents a 16% contribution of the same sign. Therefore, the first term in (B9) is the dominant one, and it can be assumed that it also determines the temperature dependence of $\Delta C_{44}$. Including the temperature dependence according to Keyes[1,2] we finally obtain the expression shown in Eq. (4). The factor $K$ for the high-concentration limit is simply

$$K = \tfrac{25}{42}(1+R) \simeq 0.69\,, \tag{B10}$$

where $R = 0.16$ represents the contribution from the second term in Eq. (B9).


[1] R. W. Keyes, IBM J. Res. Dev. 5, 266 (1961).
[2] R. W. Keyes, in *Solid State Physics*, edited by F. Seitz and D. Turnbull (Academic, New York, 1967), Vol. 20, p. 37.
[3] W. P. Mason and T. B. Bateman, Phys. Rev. 134, A1387 (1964).
[4] Einspruch and P. Csavinszky, Appl. Phys. Lett. 2, 1 (1963).
[5] J. J. Hall, Phys. Rev. **161**, 756 (1967).
[6] V. M. Beilin, Yu. Kh. Vekilov, and D. M. Krasil'nikov, Fiz. Tverd. Tela **12**, 684 (1968) [Sov. Phys.-Solid State 12, 531 (1970)].
[7] T. A. Fjeldly, in *Proceedings of the Eleventh International Conference on the Physics of Semiconductors, Warsaw, 1972*, (P.W.N-Polish Scientific Publishers, Warsaw, 1972), p. 245.
[8] G. L. Bir and A. Tursunov, Fiz. Tverd. Tela **4**, 2625 (1962) [Sov. Phys.-Solid State **4**, 1925 (1963)].
[9] P. Csavinszky and N. G. Einspruch, Phys. Rev. **132**, 2434 (1963).
[10] E. O. Kane, J. Phys. Chem. Solids **1**, 82 (1956).
[11] F. Cerdeira and M. Cardona, Phys. Rev. B **5**, 1440 (1972).
[12] T. A. Fjeldly, F. Cerdeira, and M. Cardona, Solid State Commun. **12**, 553 (1973).
[13] F. Cerdeira, T. A. Fjeldly, and M. Cardona, following paper, Phys. Rev. B 8, 4734 (1973).
[14] E. Papadakis, J. Acoust. Soc. Am. **42**, 1045 (1967).
[15] F. H. Pollak and M. Cardona, Phys. Rev. **172**, 816 (1968).
[16] F. Cerdeira, C. J. Buchenauer, F. H. Pollak, and M. Cardona, Phys. Rev. B **5**, 580 (1972).
[17] D. G. Dresselhaus, A. F. Kip, and C. Kittel, Phys. Rev. **98**, 368 (1955).
[18] F. Cerdeira, Ph.D. thesis (Brown University, 1972) (unpublished).
[19] L. D. Laude, F. H. Pollak, and M. Cardona, Phys. Rev. B **3**, 2623 (1971).
[20] J. C. Hensel and G. Feher, Phys. Rev. **129**, 1041 (1963).